General Disclaimer

One or more of the Following Statements may affect this Document

- This document has been reproduced from the best copy furnished by the organizational source. It is being released in the interest of making available as much information as possible.

- This document may contain data, which exceeds the sheet parameters. It was furnished in this condition by the organizational source and is the best copy available.

- This document may contain tone-on-tone or color graphs, charts and/or pictures, which have been reproduced in black and white.

- This document is paginated as submitted by the original source.

- Portions of this document are not fully legible due to the historical nature of some of the material. However, it is the best reproduction available from the original submission.

NASA TECHNICAL MEMORANDUM

NASA TM X-73570

NASA TM X-73570

APPLICATION OF REMOTE THERMAL SCANNING TO THE NASA ENERGY CONSERVATION PROGRAM

by Robert L. Bowman and John R. Jack
Lewis Research Center
Cleveland, Ohio 44135

January 1977

1. Report No.	2. Government Accession No.	3. Recipient's Catalog No.
NASA TM X-73570		

4. Title and Subtitle	5. Report Date
APPLICATION OF REMOTE THERMAL SCANNING TO THE NASA ENERGY CONSERVATION PROGRAM	January 1977
	6. Performing Organization Code

7. Author(s)	8. Performing Organization Report No.
Robert L. Bowman and John R. Jack	E-9017
	10. Work Unit No.

9. Performing Organization Name and Address	11. Contract or Grant No.
Lewis Research Center National Aeronautics and Space Administration Cleveland, Ohio 44135	
	13. Type of Report and Period Covered
12. Sponsoring Agency Name and Address	Technical Memorandum
National Aeronautics and Space Administration Washington, D.C. 20546	14. Sponsoring Agency Code

15. Supplementary Notes

16. Abstract

Airborne thermal scans of all NASA centers were made during 1975 and 1976. The remotely sensed data were used to identify a variety of heat losses, including those from building roofs and central heating system distribution lines. Thermal imagery from several NASA centers is presented to demonstrate the capability of detecting these heat losses remotely. Many heat loss areas located by the scan data have been verified by ground surveys. At this point, at least for such energy-intensive areas, thermal scanning has proven to be an excellent means of detecting many possible energy losses.

17. Key Words (Suggested by Author(s))	18. Distribution Statement
Energy conservation Thermal mapping Scanners Imagery	Unclassified - unlimited STAR Category 43

19. Security Classif. (of this report)	20. Security Classif. (of this page)	21. No. of Pages	22. Price*
Unclassified	Unclassified	24	A02

* For sale by the National Technical Information Service, Springfield, Virginia 22161

APPLICATION OF REMOTE THERMAL SCANNING TO THE NASA ENERGY CONSERVATION PROGRAM

by Robert L. Bowman and John R. Jack

Lewis Research Center

SUMMARY

Airborne thermal scans of all NASA centers were made during 1975 and 1976. The remotely sensed data were used to identify a variety of heat losses, including those from building roofs and central heating system distribution lines. Thermal imagery from several NASA centers is presented to demonstrate the capability of detecting these heat losses remotely. Many heat loss areas located by the scan data have been verified by ground surveys. At this point, at least for such energy-intensive areas, thermal scanning has proven to be an excellent means of detecting many possible energy losses.

INTRODUCTION

An energy conservation program has been in effect at all NASA centers for several years. As a part of this program, airborne thermal scans of all NASA centers were considered for locating areas of possible excessive energy loss.

In March 1975, a thermal scan of the Lewis Research Center was made and numerous energy losses were identified (refs. 1 and 2). Typical energy losses discovered included losses from building roofs, central heating system distribution lines, and roof ventilators. These results were presented to the NASA Energy Reduction Coordinators Conference (ref. 2) in June 1975. As a result of the interest generated at this meeting in energy loss detection by this method, a NASA-wide thermal scan program was established.

This report presents a brief introduction to infrared thermal scanning primarily for the nontechnical user, discusses its application to the detection of energy losses in energy-intensive installations, and presents some typical experimental results. Results of ground surveys based on the remotely sensed data are also presented.

INFRARED RADIATION AND ITS REMOTE DETECTION

The technique of determining the temperature of a material by remotely measuring the radiation emitted by the material has been widely used for many years (refs. 3 to 5). The purpose of this section is to present a brief background discussion for the nontechnical reader on infrared radiation and its remote detection.

All material things, by virtue of their temperature, continuously emit infrared radiation because of the thermal agitation of the atoms or molecules making up the material. The total amount and wavelength distribution of this emitted energy is dependent on the temperature and radiative efficiency (emittance) of the material. Perfect emitters (blackbodies) radiate energy according to a well-known relationship derived by Planck, which is shown in figure 1 for several temperatures. At each wavelength, the higher the temperature the greater is the energy emitted. Thus, a measurement of the energy emitted by a blackbody at any wavelength can be used to determine its temperature. Of course, all real objects are not perfect emitters and will emit less energy at each wavelength than a blackbody at the same temperature. At each wavelength, the ratio of the energy emitted by a real object to the energy emitted by a blackbody at the same temperature is the spectral emittance of the object. For a real object, as well as for the blackbody, the higher the temperature the greater is the energy emitted. Therefore, if the emittance of the object is known, a measurement of the energy emitted can be used to determine its temperature. These relationships form the basis for thermal scanning.

In general, optical systems used to measure thermal energy will only respond to radiation in particular wavelength regions. Optical systems must then be selected that will measure radiant energy in the wavelength region of maximum interest. Figure 1 shows that the maximum energy emitted by a blackbody at temperatures in the region of interest (300 K) for thermal scanning occurs at wavelengths in the neighborhood of 10 micrometers. Thus, a detector and optical system that will operate in this wavelength region is desirable.

An additional factor that affects the remote measurement of thermal radiation is atmospheric absorption. Some atmospheric gases, in particular water vapor and carbon dioxide, absorb energy in the infrared region. Consequently, thermal scans can only be made at wavelengths where the transmittance of the atmosphere is high (low absorption). A typical spectral transmittance curve of the atmosphere is shown in figure 2. The transmittance is high between 3 and 5 micrometers and between 8 and 14 micrometers. The actual transmittance depends on the quantity of absorbing gases between the source and the detector. Since the maximum emitted energy for temperatures of interest occurs at 10 micrometers and the transmission of the atmosphere is high at that wavelength, detectors and scanning systems are used that operate efficiently

in the 8- to 14-micrometer range.

A variety of detectors are available that operate in this range. The relative spectral response of a typical thermal detector (mercury-cadmium-telluride) is shown in figure 3(a) along with the response of other detectors for comparison. The HgCdTe detector responds well to radiation between 4 and 14 micrometers. Since a detector's response is dependent on the temperature difference between the source and the detector, the detector is normally cooled to liquid-nitrogen temperatures (77 K) to achieve a high signal-to-noise ratio (fig. 3(b)).

For remote sensing, an optical system that operates in a scan mode, somewhat analogous to a television camera, is frequently used. A device such as a rotating mirror or prism is used to scan the ground along the flight path and to direct the radiation into a detection system. The signal from the detection system can then be used to reconstruct an image of the scene on the ground.

The thermal imagery used in this program was obtained from the thermal band of a modular multiband scanner (M^2S) mounted in the Lewis C-47 aircraft. A schematic of the scanning and detection system for the thermal band of the M^2S is shown in figure 4. The rotating mirror scans a path on the ground perpendicular to the direction of flight with a total angular field of view of 115°. This gives a scan width of 956 meters per 305 meters of altitude (3140 ft/1000 ft) above the ground. The instantaneous field of view is 2.5×10^{-3} radian - which, at nadir, gives a square ground resolution element (pixel) of 0.76 meter per 305 meters of altitude (2.5 ft/1000 ft).

Radiation from a pixel is reflected by the scan mirror into a telescope that focuses the energy into the detector section (fig. 4). Thermal infrared radiation is then reflected by the dichroic filter to an infrared filter that transmits radiation between 8 and 12 micrometers to the liquid-nitrogen-cooled HgCdTe detector. The detector produces a time-varying signal corresponding to the intensity of the thermal energy from the pixels along a scan line. This signal is recorded on magnetic tape. The scan rate (rotational speed of the scan mirror) is adjusted so that for a given speed and altitude, the aircraft moves forward exactly one swath width (fig. 4) for each revolution of the scan mirror. The data for each scan line are stored sequentially on magnetic tape. In this way, the M^2S system records thermal data from which a continuous thermal map of the Earth's surface can be reconstructed.

To establish reference temperatures for the thermal data, the rotating mirror scans two temperature-controlled blackbodies within the scanner (fig. 4). These blackbodies can be set at temperatures between -10° C (14° F) and 40° C (106° F). In general, they are set so that the scene temperatures lie between the two reference temperatures, which are also recorded on magnetic tape with each scan line. If we assume a linear relationship between radiation energy and temperature as established by the two reference blackbodies, the effective radiation temperature for detected

energy lying within this range can be determined. (This assumption of a linear relationship is valid for the scanner calibration temperature range.) If the surface band emittance is known, the true surface temperature T_s can be calculated from the effective radiation temperature T_{eff} by the following approximate expression:

$$T_s = \frac{T_{eff}}{(\epsilon_{band})^{1/4}} \tag{1}$$

where ϵ_{band} is the average emittance of the material over the M^2S wavelength band (8 to 12 μm) and the temperatures are absolute (e.g., K = ^{o}C + 273). For energy losses of interest, the band emittances are generally greater than 0.7, and the maximum temperature error from the use of equation (1) rather than the exact expression is 2 percent.

PROCEDURE

Thermal scans of all the NASA centers were taken between March 1975 and April 1976, as summarized in table I. With the exception of three centers, all of the data flights were made at night to minimize the effects of solar heating. The Wallops Flight Center and Langley Research Center flights were made in the late afternoon because a storm system was moving into the area. These two centers had been under cloud cover most of the day so that the effects of solar heating should be minimal. At the National Space Technology Laboratory the flight was made in the morning to maximize the temperature difference between the ground and the heating pipes of interest. In general, the flights were made at altitudes of either 305 or 457 meters (1000 or 1500 ft) above the terrain. However, in a few cases, topographical features required other flight altitudes.

The signals from the thermal detector were digitized into 256 levels and recorded on high-density magnetic tape on board the aircraft. The data were then analyzed at a later date on a ground-based minicomputer system programmed to divide the 256 digital levels into 24 levels for display and analysis. Of these 24 levels, the first one contained all data less than a selected value and the last one contained all data higher than a selected value. The digital data between the two selected levels were divided into 22 equal increments. An effective temperature range was assigned to each interval by using the data from the two reference blackbodies. The low-temperature level and the increments were selected by considering the basic scene temperature and the temperature sensitivity required to identify accurately the energy losses of interest. For ex-

ample, analysis of rooftops for energy losses may require more temperature discrimination than detecting losses in underground steam lines. Thus, the same scene may be processed using several different temperature intervals depending on the user's requirements.

Our experience showed processed data from the minicomputer system in four different formats to be useful for detecting energy losses, namely,

(1) Twenty-four level color imagery from the system image recorder
(2) Twelve-level black-and-white imagery from the system image recorder
(3) Thirty-five millimeter color photography of the minicomputer systems cathode-ray-tube (CRT) display
(4) Minicomputer system printout of the digital data

For example, a color image of the Lewis Research Center taken from an altitude of 457 meters (1500 ft) is shown in figure 5, with each color representing an effective temperature range of about 0.7° C. This type of image is useful in obtaining an overall view of the scene and in locating heat loss areas. However, even with photoenlargement (four times the film recorder negative) shown in the figure, detailed analysis of a particular heat loss area is not possible.

A black-and-white film image with 12 density levels having temperature intervals twice as large as for the color image was effective in locating energy loss areas. Figure 6 is a 12-level black-and-white image of Lewis showing the same scene as figure 5. In the figure, black represents the lowest temperature and white the highest. According to several users, the black-and-white imagery was easier to use than the color imagery for locating and identifying heat loss areas. The black-and-white imagery was easier to use because there were fewer levels to differentiate and hence the contrast was increased. Since black-and-white imagery was the least expensive to generate and could also be obtained in the shortest time, it was generally used to locate heat loss areas that required more-detailed analysis.

For more-detailed analysis of a particular heat loss area, the selected area was displayed on a color television monitor (CRT) associated with the minicomputer system. The colors and temperature intervals used for the display were the same as those used for the color film image. On the CRT, individual pixels (ground resolution elements) could be observed that could not be seen on the film imagery. Color photographs of the CRT were taken that allowed detailed analysis of the selected areas of excessive heat loss. All imagery presented herein, except for figures 5 and 6, was obtained in this manner.

The most-detailed analysis format used was to print out the digital data (256 levels possible) for each pixel in an area of particular interest to the user. The area of interest can easily be selected and designated by interacting with the CRT monitor. Because of the expense involved, digital printouts were obtained only in unique situations

where very detailed information on a particular energy loss area was required to meet a user's special needs.

USER INTERACTION AND DATA TRANSFER

Thermal scan flights were made by the Lewis aircraft with the cooperation of personnel at each NASA facility. Each center supplied site plans for flight planning and also indicated areas of particular concern for energy losses. Heating systems were left in full daytime operation until the flights were completed so that the energy losses to be detected were a maximum.

All data were processed by Lewis personnel using a leased minicomputer system. Possible energy loss areas were located on the black-and-white film imagery. Color photographs of the television monitor that were taken of each energy loss area were identified on the black-and-white imagery for the user. At this point, the data were transferred and each center was then responsible for heat loss verification and determination of possible corrective action, if any, to be taken.

RESULTS AND DISCUSSION

Only selected results from the thermal scans of the various centers are presented in this report. These results are typical and demonstrate the use of thermal scanning to locate possible energy losses from roofs, ventilator fans in operation, and central heating system distribution lines. In several cases, a very simplified approximation to the quantitative heat loss is also presented.

At the National Space Technology Laboratory (NSTL), the primary concern was to locate heat losses in over 13 miles of underground high-temperature hot water (HTHW) lines. Both supply and return lines for the HTHW system are buried from 1.2 to 3.0 meters (4 to 10 ft) underground, with an average depth of 1.8 meters (6 ft). They are insulated with a calcium silicate material with an air space and a steel outer casing, a pipe insulation system commonly known as Rickwell. A section of the HTHW lines in the vicinity of one of the powerplants, as seen in the infrared imagery, is shown in figure 7. The diameters of the buried pipes (20.3 to 25.4 cm (8 to 10 in.)) are less than the resolution capability of the scanner. Even so, their location can be clearly seen on the imagery because the heat lost from the pipes flows radially through the ground and affects a large enough area on the surface to be seen by the scanner. The locations of the lines, along with expansion joints and manhole covers, are identified in the figure. The white areas in the figure indicate effective radiation tempera-

tures higher than 29.8° C (85.7° F). Thus, there are large heat losses due either to leaks in the lines or to deteriorated insulation. The high effective temperatures (yellow) found over much of the lines are, in all probability, due to deteriorated insulation resulting from the high ground water table. The ability to evaluate energy losses from underground HTHW lines from remotely sensed data has resulted in considerable savings over the conventional spot-check method, which includes excavation at selected locations. For example, at NSTL, the cost of a proposed conventional survey of the 13-mile HTHW system was estimated to be $100 000 (NASA memorandum from the Director of Technology Applications Programs to the Associate Administrator for Applications, Dec. 1, 1975). The cost of thermal scanning the entire system was $7000. Thus, the cost savings for evaluating the complete central heating system of just one NASA center was about $93 000.

At the Marshall Space Flight Center (MSFC) the central heating distribution system was also of major concern. The MSFC system contains both underground lines similar to those at NSTL and above-ground lines. Examples of both types of lines are shown in figure 8. The white areas show losses from the underground lines at effective radiation temperatures greater than 21.0° C (69.9° F). An interesting energy loss can be observed in the center of the figure, where the line goes under a divided highway. The top section is at a higher effective temperature over a much larger area than the lower section. The explanation for this is that the section having the lower effective temperature had been repaired prior to the flight. Even with the repair, considerable energy is still being lost.

An excellent example of the effect of material emittance on effective temperature is shown in figure 8. The above-ground steam lines appear colder than the background. In this case, however, the lines are encased in aluminum, which has a very low emittance. Therefore, the true temperature of the lines would be much greater than indicated in the figure. However, comparing effective temperatures of materials with about the same emittance, such as the road areas discussed previously or roofs, still provides a relative indication of excessive heat loss.

At the Lewis Research Center the steam distribution lines are in tunnels along with other utilities. A section of the surface over the utility tunnel is shown in figure 9(a), and an expanded view of a portion of figure 9(a) is shown in figure 9(b). The road over the tunnel shows effective temperatures as high as 17.8° C (64.0° F) in contrast to other sections of the line, which have effective temperatures between 4.1° and 5.0° C (39.4° and 41.0° F). The higher temperatures indicate heat losses in the steam distribution system at these locations.

The white area to the left of the road (figs. 9(a) and (b)) is a hood housing a 382-cubic-meter-per-minute (13 500-ft^3/min) exhaust fan used to ventilate a portion of the tunnel. The white color in the vicinity of the fan represents effective temperatures of

19.8° C (67.6° F) or higher. With the measured ambient temperature, 5.6° C (42.0° F), the minimum amount of heat lost through this ventilator can be calculated as follows:

$$\text{Heat lost from ventilator exhaust} = \rho c_p \dot{\omega} \Delta T$$

where

ρ density of air

c_p specific heat of air

$\dot{\omega}$ volume flow rate of air

ΔT temperature difference between heated air and ambient temperature

This calculation shows that a minimum of 118 kilowatts (403 000 Btu/hr) is being lost through this one ventilator. There are a number of ventilator fans of different capacities ventilating this tunnel. Also, the temperature difference used in this calculation is a minimum value and the heat lost by conduction through the tunnel walls to the ground has not been included in the calculation. As a result, the total heat being lost from the tunnel system is no doubt considerably more than the calculation indicates.

In figure 9(a), the warm areas on the roofs of the Lewis PSL Engine Test Building and the Zero-Gravity Facility indicate that a number of building exhaust fans were in operation during the flight. The exhaust fans on the PSL Engine Test Building are rated at 325 cubic meters per minute (11 500 ft^3/min) so that, as indicated by the tunnel ventilator calculation, considerable amounts of heat can be lost if such roof fans are operated unnecessarily.

Thermal imagery of the 10- by 10-Foot Supersonic Wind Tunnel office and computer center at Lewis taken March 17, 1975, is shown in figure 10. The white area represents the entrance steps to the building. These steps are electrically heated with a heater rated at 16.5 kilowatts to prevent ice and snow buildup. Even though the temperature was above freezing with clear weather at the time of flight, the high effective temperatures measured (>19.1° C (66.4° F)) indicate that the heater was operating that night. Thus, inadvertently, 16.5 kilowatts of energy (56 336 Btu/hr) was being consumed unnecessarily.

Figure 11(a) shows an area of high temperature and large temperature gradients on the roof of the Lewis Refrigeration Building. A subsequent ground investigation showed that this roof area was heated by a leak in a steam line running along the edge of the roof. The leak was repaired, and a later thermal scan showed a uniform roof temperature (fig. 11(b)).

Figure 12 is a thermal image of the Visitor Information Center at the Langley Research Center. One corner of the building is obviously losing excessive heat. It has an effective radiation temperature of approximately 2.0° C (35.6° F), while the cooler sections of the same roof have effective temperatures of about -2.0° C (28.4° F). Even though the temperature difference is relatively small in this case, it still represents a sizable heat loss because of the large amount of area involved.

The roof of a warehouse at the Goddard Space Flight Center is shown in figure 13. Here the red areas represent effective temperatures between -5.5° C (22.1° F) and -4.9° C (23.2° F). The predominantly green areas represent effective temperatures between -13.3° C (8.1° F) and -13.9° C (7.0° F). The heat losses per unit area associated with these areas can be calculated by

$$q_{red} = k\left(\frac{T_{red}}{\epsilon^{1/4}} - T_a\right)$$

$$q_{green} = k\left(\frac{T_{green}}{\epsilon^{1/4}} - T_a\right)$$

where

k	surface conductance including convective and radiative heat transfer (ref. 6)
ϵ	surface band emissivity (assumed to be constant)
T_{red}, T_{green}	effective radiation temperatures of red and green areas (absolute units)
T_a	measured ambient air temperature (absolute units)

Thus, using a band emittance of 0.9 for the roof (which appears to be a reasonable value for this type of roof) and taking a ratio of heat losses to eliminate the unknown parameter k show the red areas to be losing 30 times more heat per square meter than the predominantly green areas.

GROUND TRUTH VERIFICATION OF TECHNIQUE

Several centers have done ground surveys to verify and study the heat loss areas indicated by the remote thermal scan data. In general, excellent agreement has been

found between the remotely obtained thermal data and the ground surveys.

For example, based on the thermal scan data, a section of NSTL's HTHW lines has been examined by excavation, pressure checking, and sulfur hexafluroide leak detection. In the section tested, the energy losses indicated by the thermal imagery were found to be due either to leaks in the HTHW lines or to water-damaged insulation (NSTL Document 368-76-043: Preliminary Engineering Report, Rehabilitation of High-Temperature Hot Water Distribution System at NSTL. National Space Technology Laboratory, April 2, 1976). At the present time, plans are being made for repair of the system.

At MSFC, several sites were excavated on the basis of the thermal scan results. The sites were selected to give examples of high-loss areas and areas of less loss as shown on the imagery. In each case, the imagery was very accurate. Predicted high-loss areas were found, when excavated, to have either no insulation or badly deteriorated insulation or to be actual leaks in the lines. Where thermal data indicated less heat loss, the insulation was found to be intact but in generally poor condition.

Extensive ground surveys at Lewis identified all possible energy loss areas seen in the thermal imagery. Sources of energy losses included roof ventilators, exhausters from research facilities, steam lines, and electrical transformers. Again, the thermal data were verified by the results of the ground surveys.

RECOMMENDATIONS AND FUTURE PLANS

At this point, thermal scanning has proven to be an excellent, cost-effective means of detecting and locating energy losses at energy-intensive installations. For example, as previously noted, the cost savings for evaluating the NSTL central heating system was about $93 000. However, in most cases, the cost benefits to be derived from thermal scanning have not been completely determined and perhaps are not as obvious as those for NSTL. Better methods are needed for quantitatively analyzing thermal imagery by taking into consideration such effects as the surface emittance on the measured temperature and, hence, on the heat flux; the temperature accuracy and discrimination on the quantitative heat flux; and flight parameters such as altitude, weather conditions, and time of day. With a method including these considerations the user could determine the energy losses indicated, estimate the cost of corrective measures, and finally determine the cost benefits involved. Such a program to develop simple procedures for determining useful, quantitative heat losses from thermal scan data and to verify these procedures is now in progress at Lewis.

SUMMARY OF RESULTS

Airborne thermal scans and thermal maps of all the NASA field centers have been made to help implement NASA's energy conservation program. All major areas of energy loss have been identified and studied. These thermal maps have been transferred to the various users at each field center, who are in the process of determining the corrective actions to be taken.

Many areas of energy loss have been identified and located from the remotely sensed thermal data, and these areas have been verified from ground surveys. To increase the value of the thermal scan data to the user, a program is being developed to make quantitative heat loss calculations from the data. Such a program will enable the user to determine the possible cost benefits to be derived from repairs.

REFERENCES

1. Jack, J. R.; and Bowman, R. L.: Application of Thermal Scanning to the NASA LeRC Energy Conservation Program. AIAA Paper 75-744, May 1975.

2. Bowman, R. L.; and Jack, J. R.: Application of Thermal Scanning to the NASA LeRC Energy Conservation Program. Paper presented to the NASA Energy Reduction Coordinators Meeting, NASA Lewis Research Center, Cleveland, Ohio, June 25, 1975.

3. Harrison, Thomas R.: Radiation Pyrometry and its Underlying Principles of Radiant Heat Transfer. John Wiley & Sons, Inc., 1960.

4. Crouch, L. W.; and Mower, R. D.: An Application of Infrared Remote Sensing Techniques to Ecological Problems. AFAL-TR-74-98, Air Force Avionics Lab. (AD-786028), 1974.

5. Bjorkland, J.; Schmer, F. A.; and Isakson, R. E.: Aerial Thermal Scanner Data for Monitoring Rooftop Temperatures. (SDSU-RSI-75-11, Remote Sensing Inst., South Dakota State Univ.; Grant NGL-42-003-007) NASA CR-145747, 1975.

6. ASHRAE Handbook of Fundamentals. Am. Soc. Heat. Refrig. Air-Cond. Eng., 1972.

TABLE I. - SUMMARY OF THERMAL SCAN FLIGHTS

Center	Date	Local time	Altitude above terrain	
			m	ft
Lewis Research Center	Mar. 17, 1975	10:20 p. m.	457	1500
National Space Technology Laboratory	Sept. 10, 1975	8:00 a. m.	457	1500
Marshall Space Flight Center	Oct. 22, 1975	11:00 p. m.	305	1000
Kennedy Space Center	Dec. 10, 1975	9:45 p. m.	305	1000
Michoud Assembly Facility	Dec. 11, 1975	10:20 p. m.	457	1500
Goddard Space Flight Center	Jan. 19, 1976	10:00 p. m.	305	1000
Wallops Flight Center	Jan. 21, 1976	5:00 p. m.	↓	↓
Langley Research Center	Jan. 21, 1976	6:30 p. m.		
Marshall Space Flight Center	Feb. 17, 1976	10:00 p. m.		
Johnson Space Center	Feb. 18, 1976	11:00 p. m.		
	Feb. 19, 1976	10:00 p. m.		
Ames Research Center	Mar. 3, 1976	10:00 p. m.		
Downey Industrial Plant	Mar. 4, 1976	9:30 p. m.	↓	↓
Jet Propulsion Laboratory	↓	9:50 p. m.	366	1200
Dryden Flight Research Center		10:30 p. m.	305	1000
Jet Propulsion Laboratory		10:45 p. m.	305	1000
Eastern Test Station				
Goldstone Tracking Station	↓	11:25 p. m.	610	2000
Lewis Research Center	Apr. 7, 1976	10:00 p. m.	305	1000
	Apr. 8, 1976	2:00 a. m.	305	1000

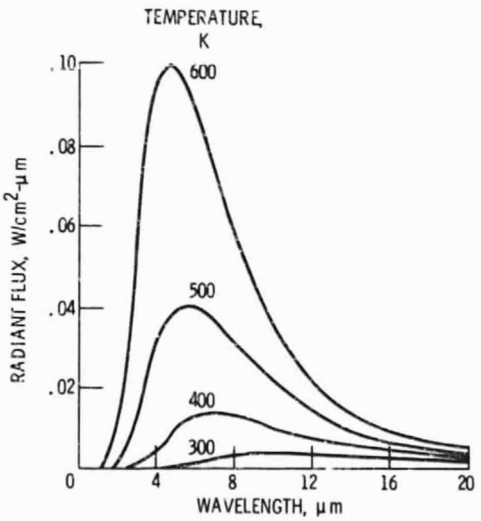

Figure 1. - Blackbody radiation spectra.

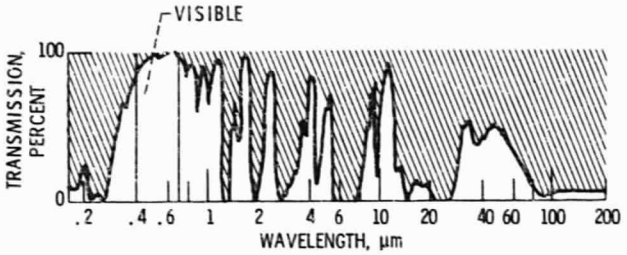

Figure 2. - Typical atmospheric transmission spectrum.

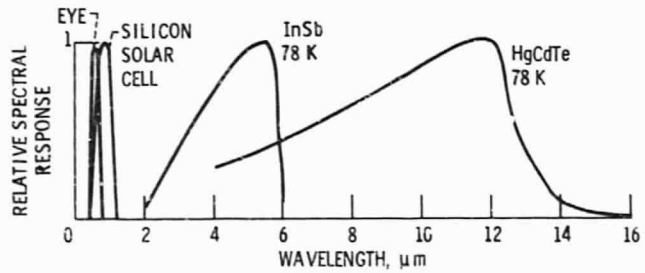

(a) Spectral response of typical detectors.

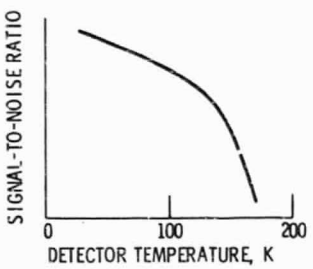

(b) Signal-to-noise ratio.

Figure 3. - Typical detector response characteristics.

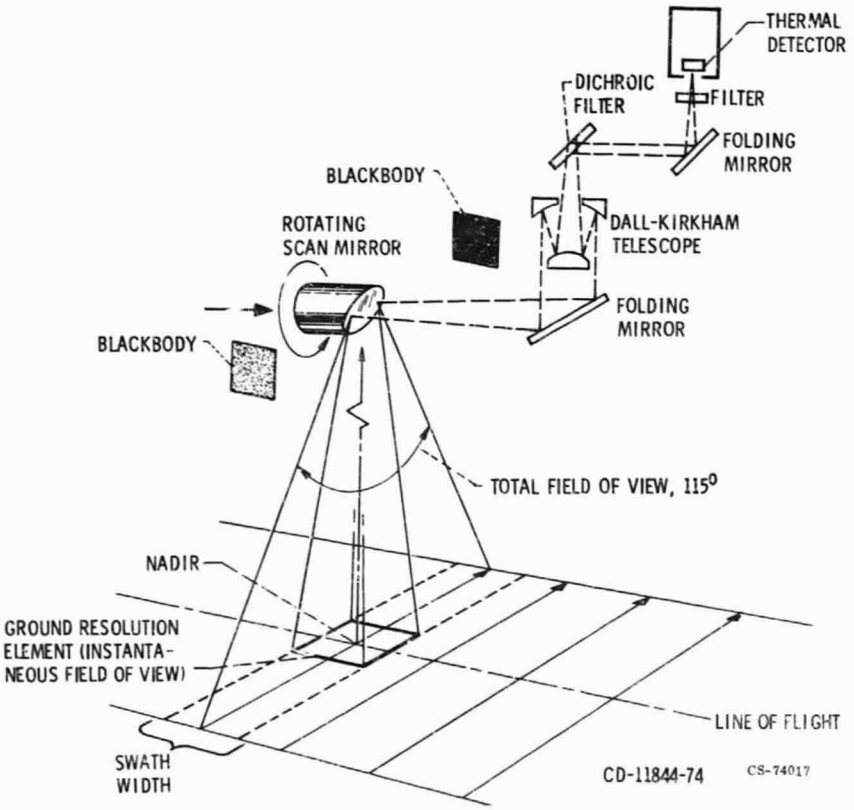

Figure 4. - Schematic of modular multiband scanner (M^2S) system.

Figure 5. - Thermal scan of Lewis Research Center, March 17, 1975 - color imagery. Altitude, 457 meters (1500 ft); ambient temperature, 5.6 °C.

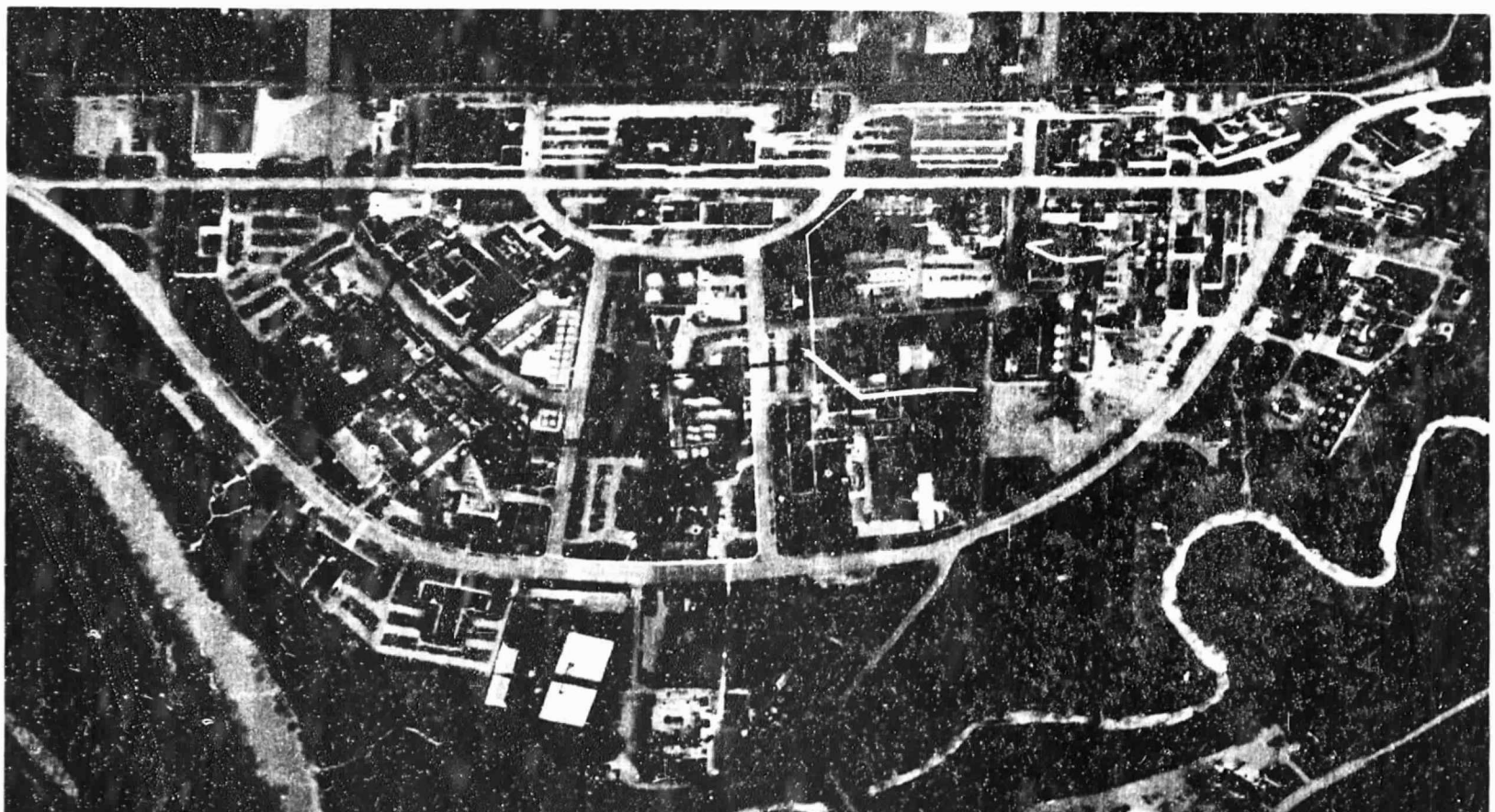

Figure 6. - Thermal scan of Lewis Research Center, March 17, 1975 - black-and-white imagery. Altitude, 457 meters (1500 ft); ambient temperature, 5.6° C.

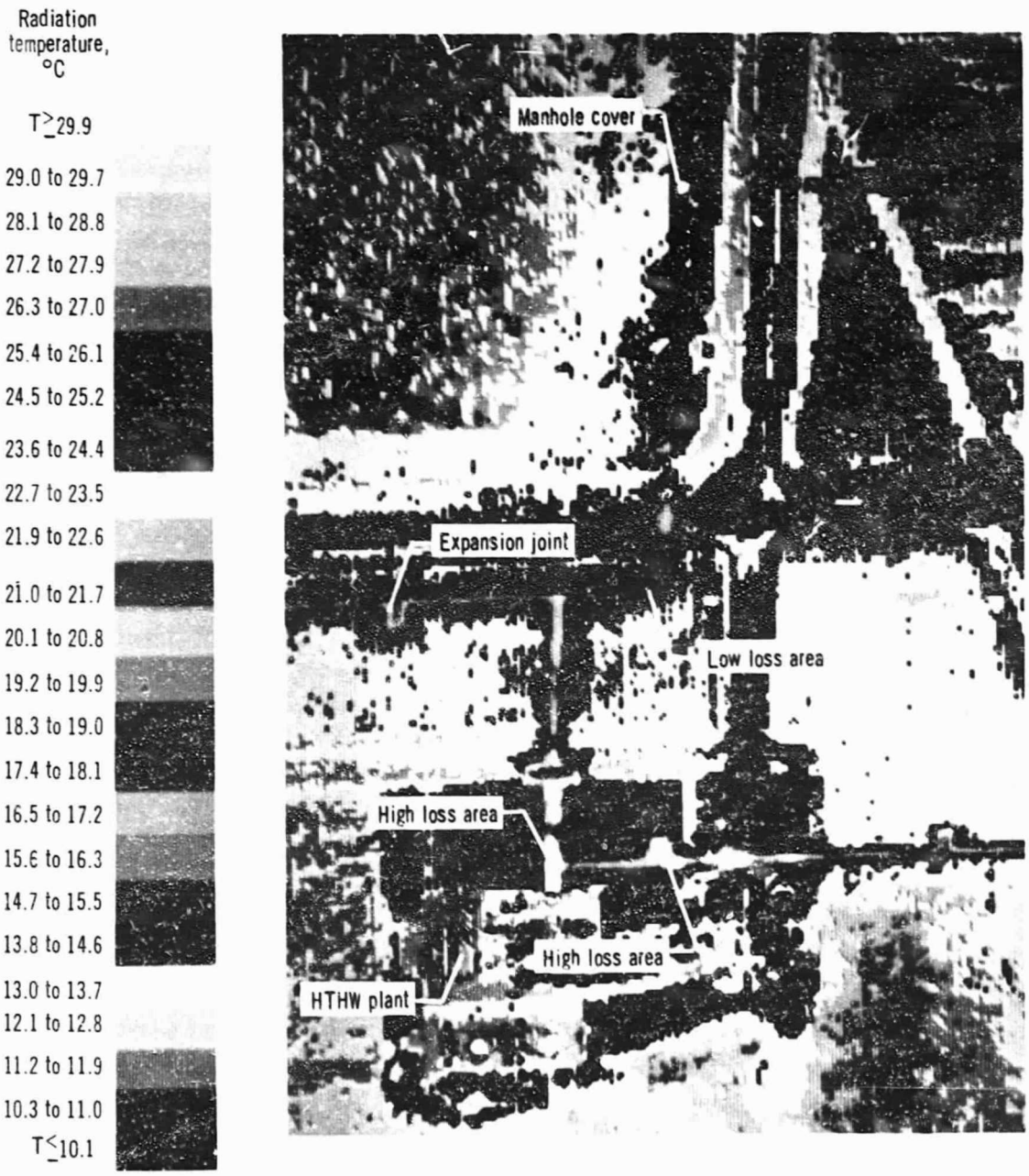

Figure 7. - Thermal scan of National Space Technology Laboratory showing section of underground high-temperature hot water (HTHW) system - September 10, 1975. Altitude, 305 meters (1000 ft); ambient temperature, 23.9° C.

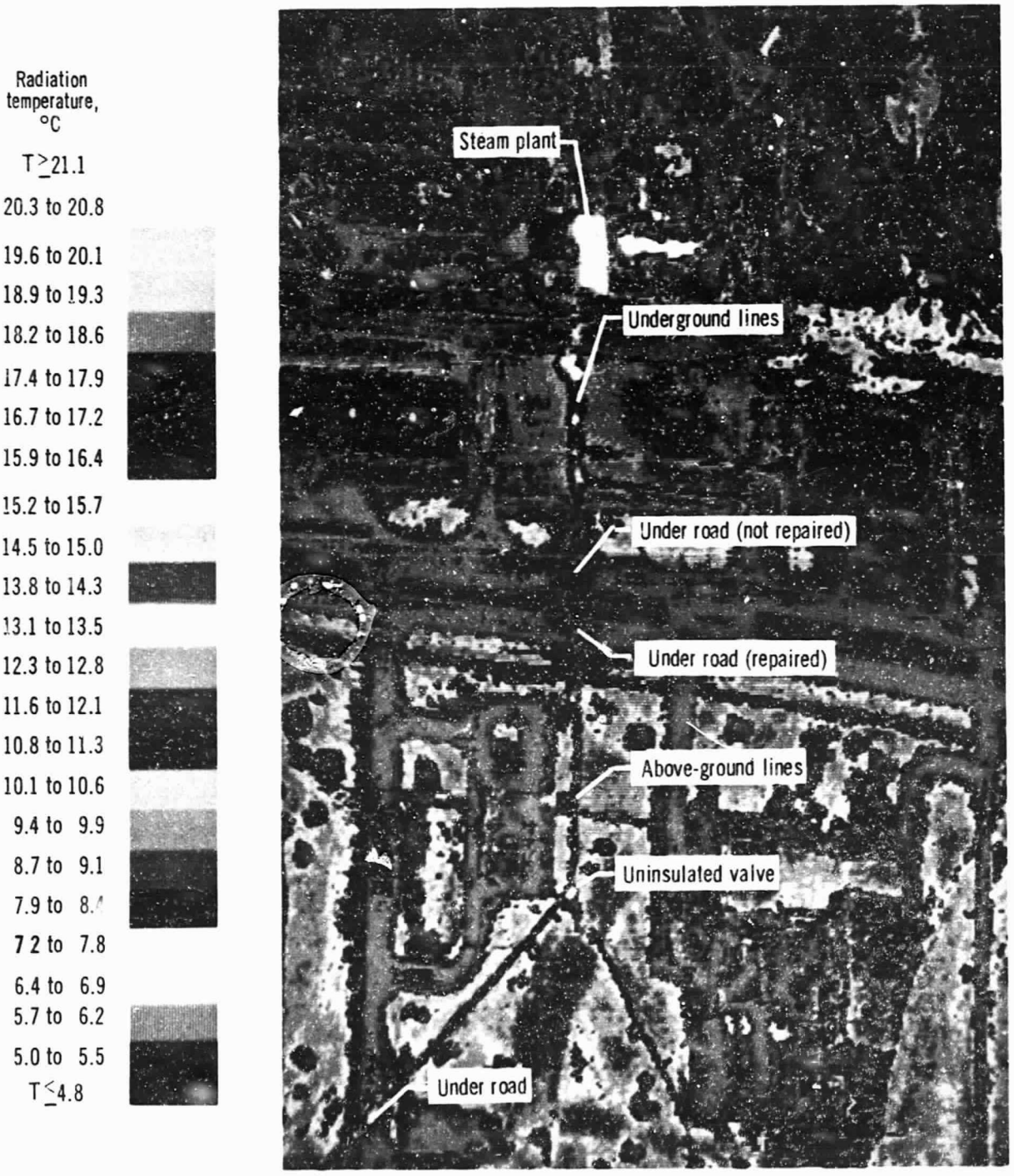

Figure 8. - Thermal scan of Marshall Space Flight Center showing section of steam distribution system - October 22, 1975. Altitude, 305 meters (1000 ft); ambient temperature, 12.2 °C.

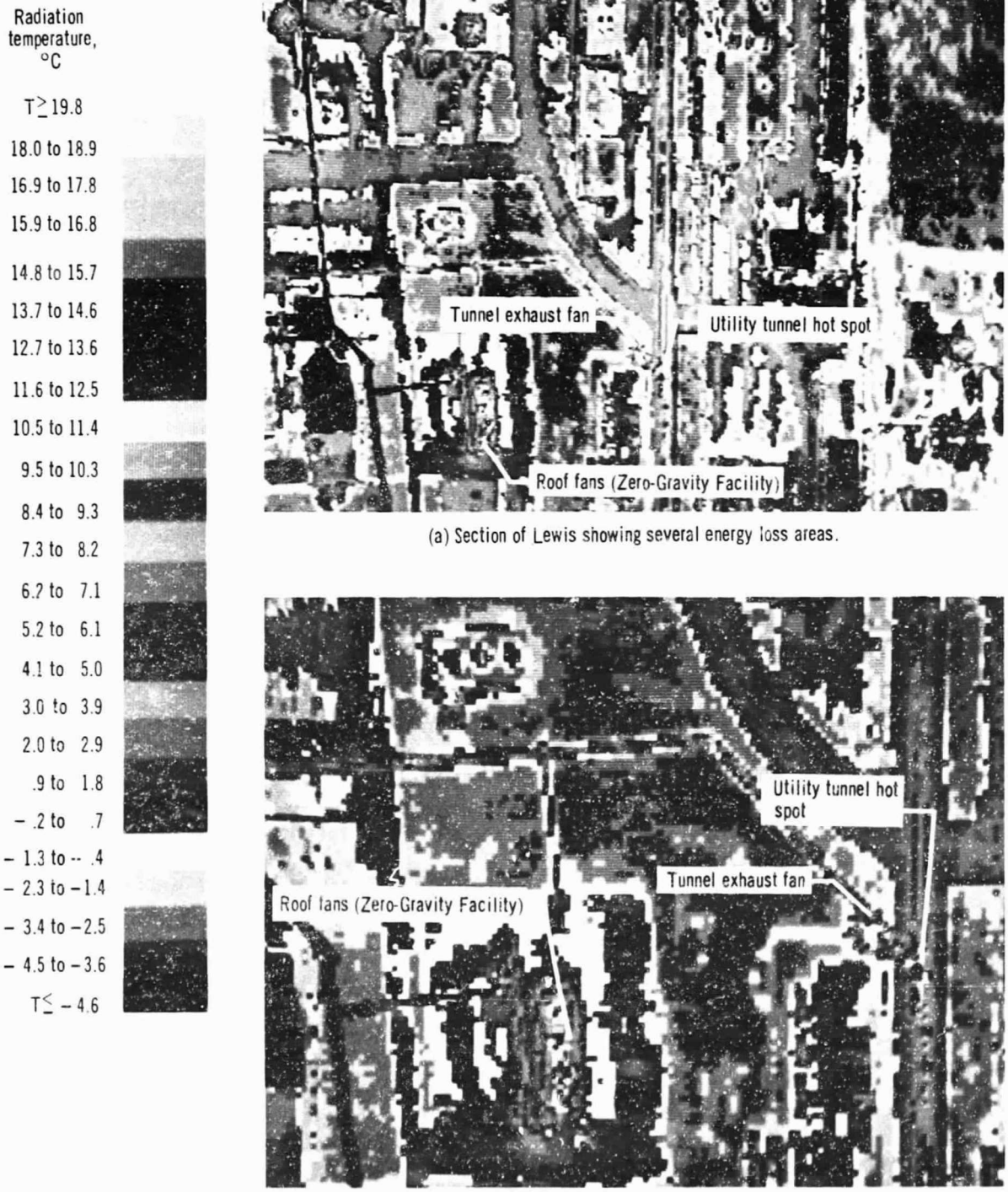

(a) Section of Lewis showing several energy loss areas.

(b) Expanded view of a portion of (a).

Figure 9. - Thermal scan of Lewis Research Center, March 17, 1975. Altitude, 457 meters (1500 ft); ambient temperature, 5.6° C.

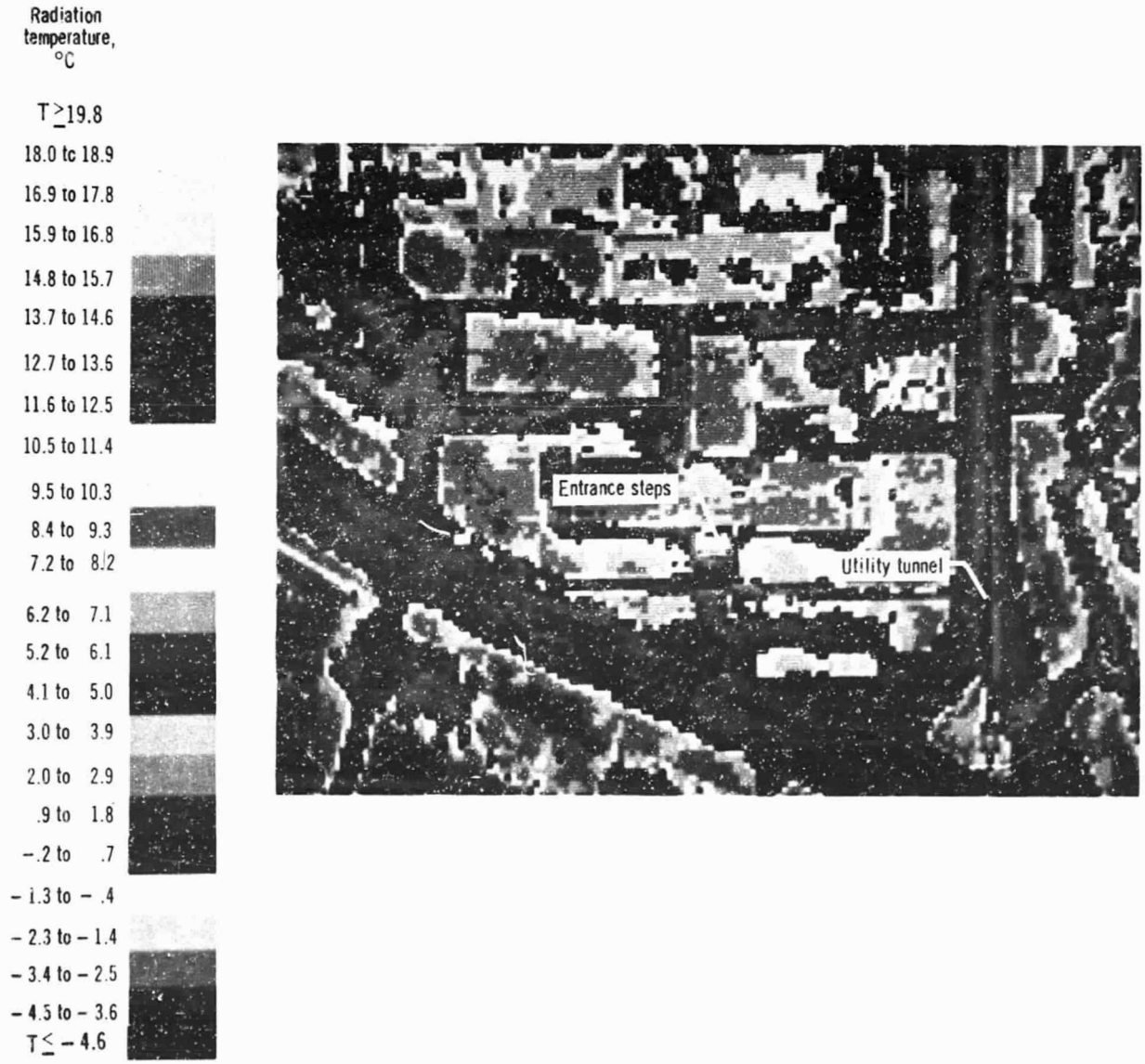

Figure 10. - Thermal scan of 10- by 10-Foot Supersonic Wind Tunnel office and computer center at Lewis Research Center - March 17, 1975. Altitude, 457 meters (1500 ft); ambient temperature, 5.6 °C.

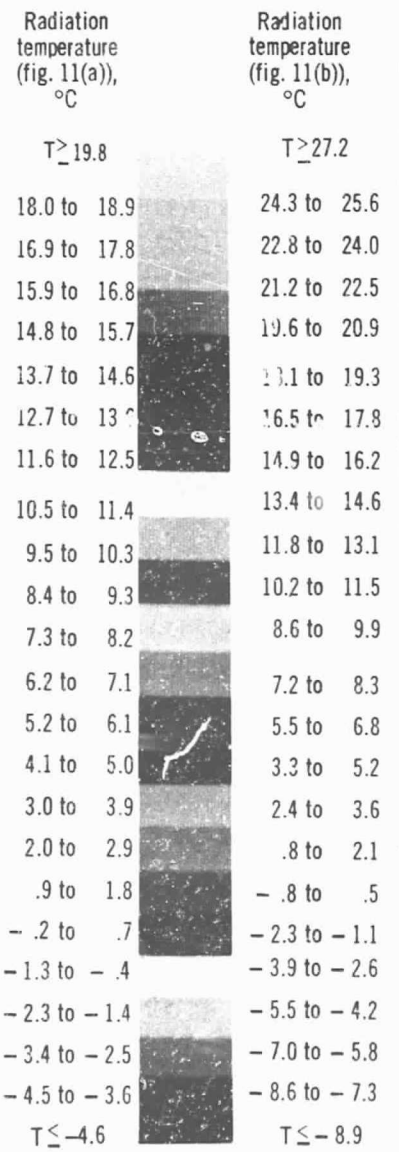

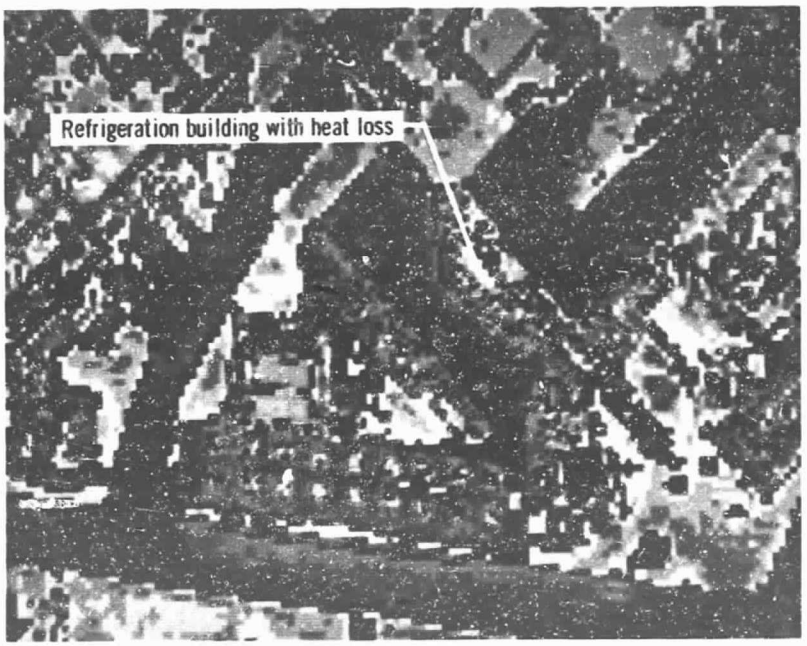

(a) Refrigeration Building showing high roof temperature from leak in steam line - March 17, 1975. Expanded view from altitude of 457 meters (1500 ft); ambient temperature, 5.6 °C.

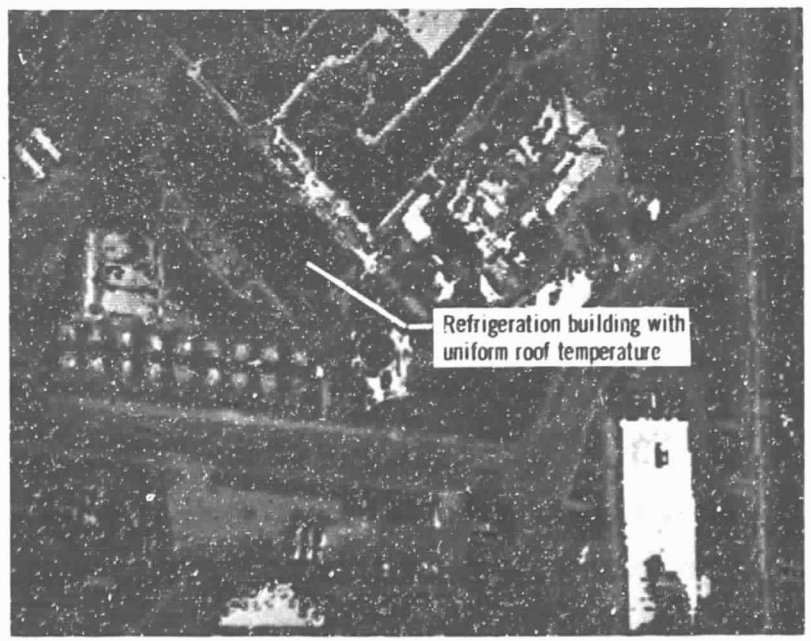

(b) Refrigeration Building showing uniform roof temperature after repair of steam leak - April 7, 1976. Altitude, 305 meters (1000 ft); ambient temperature, 3.3 °C.

Figure 11. - Thermal scans of Lewis Research Center Refrigeration Building showing effect of steam leak and repair on roof temperature.

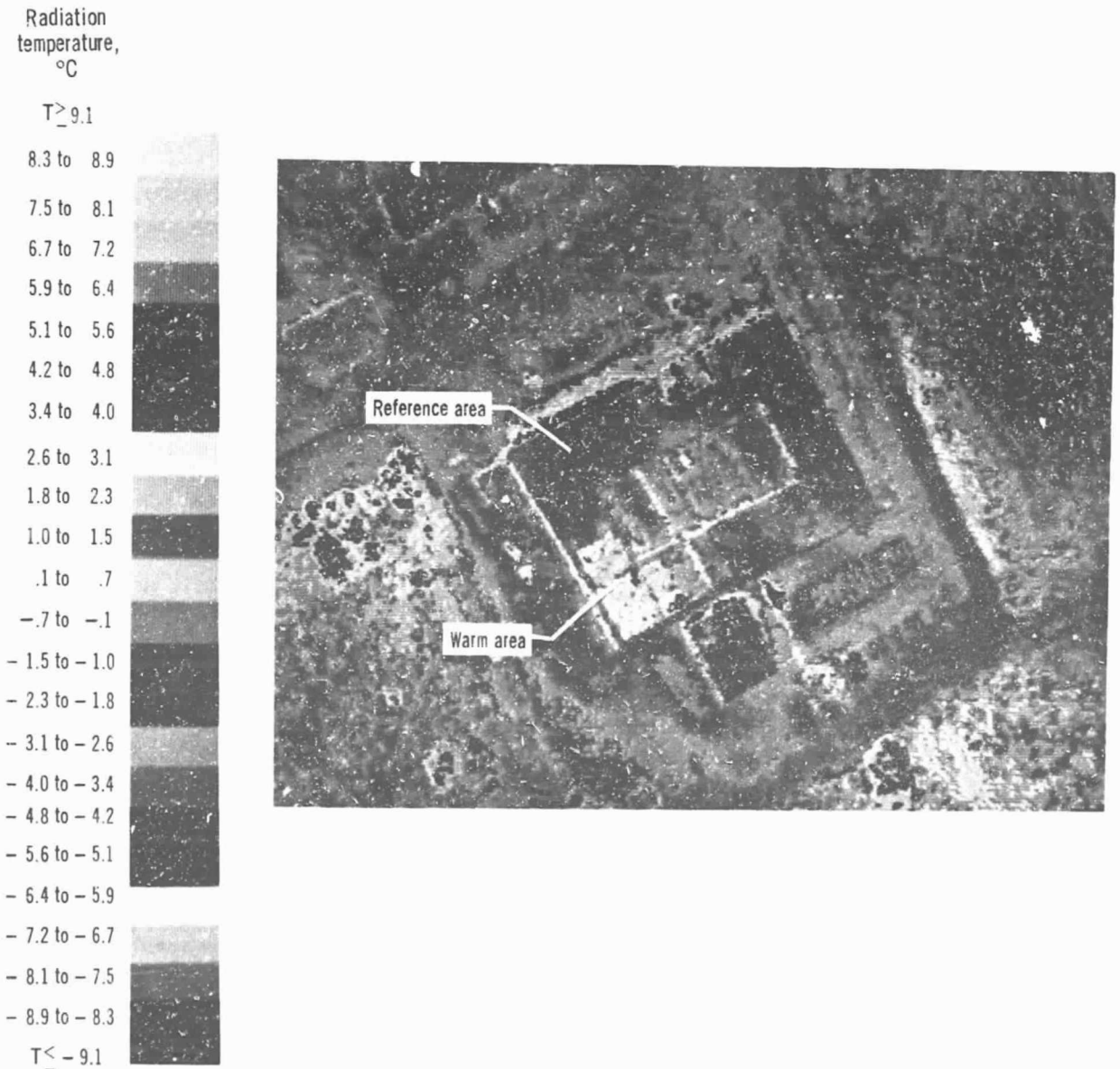

Figure 12. - Thermal scan of Visitor Information Center at Langley Research Center. Altitude, 305 meters (1000 ft); ambient temperature, 7.8° C.

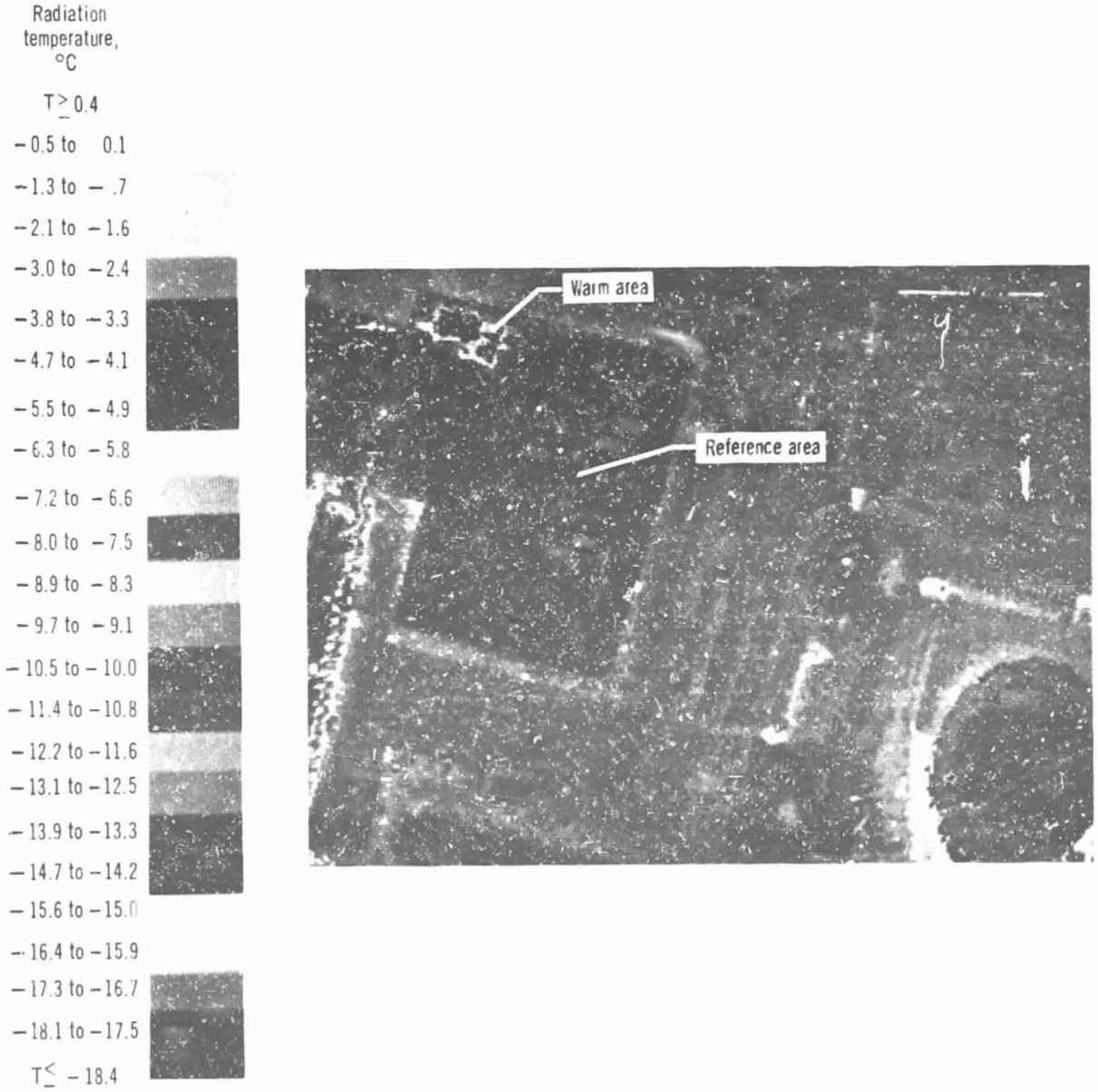

Figure 13. - Thermal scan of warehouse at Goddard Space Flight Center - January 19, 1975. Altitude, 305 meters (1000 ft); ambient temperature, – 6.7° C.